

A NEW MULTIPOINT SYMMETRIC SECANT METHOD WITH A DENSE INITIAL MATRIX

JENNIFER B. ERWAY AND MOSTAFA REZAPOUR

ABSTRACT. In large-scale optimization, when either forming or storing Hessian matrices are prohibitively expensive, quasi-Newton methods are often used in lieu of Newton’s method because they only require first-order information to approximate the true Hessian. Multipoint symmetric secant (MSS) methods can be thought of as generalizations of quasi-Newton methods in that they attempt to impose additional requirements on their approximation of the Hessian. Given an initial Hessian approximation, MSS methods generate a sequence of possibly-indefinite matrices using rank-2 updates to solve nonconvex unconstrained optimization problems. For practical reasons, up to now, the initialization has been a constant multiple of the identity matrix. In this paper, we propose a new limited-memory MSS method for large-scale nonconvex optimization that allows for dense initializations. Numerical results on the CUTEst test problems suggest that the MSS method using a dense initialization outperforms the standard initialization. Numerical results also suggest that this approach is competitive with both a basic L-SR1 trust-region method and an L-PSB method.

DEDICATION

This paper is dedicated to Oleg Burdakov who passed away June 1, 2021.

1. INTRODUCTION

We consider nonconvex large-scale unconstrained optimization problems of the form

$$\min f(x), \tag{1}$$

where $f : \mathfrak{R}^n \rightarrow \mathfrak{R}$ is a twice-continuously differentiable function. In this setting, second-order methods are undesirable when the Hessian is too computationally expensive to compute or store. In this paper, we consider the first-order multipoint symmetric secant (MSS) method [1] and its limited-memory extension [2]. We propose a new formulation of the limited-memory MSS method that allows for a dense initialization in place of the usual scalar multiple of the identity matrix. The dense initialization does not significantly increase storage costs; in fact, the dense initialization only requires storing one extra scalar.

Multipoint symmetric secant methods can be thought of as generalizations of quasi-Newton methods. Quasi-Newton methods generate a sequence of possibly-indefinite matrices $\{B_k\}$ to approximate the true Hessian of f . These methods build Hessian approximations using *quasi-Newton pairs* $\{s_k, y_k\}$ that satisfy the *secant*

Key words and phrases. Quasi-Newton methods; large-scale optimization; nonlinear optimization; trust-region methods .

J. B. Erway is supported in part by National Science Foundation grant IIS-1741264.

condition $B_{k+1}s_k = y_k$ for all k . In contrast, MSS methods seek to impose the secant condition on *all* the stored pairs: $B_k S_k = Y_k$ for all k , where

$$S_k = [s_{k-1} \ s_{k-2} \ \dots \ s_0] \quad \text{and} \quad Y_k = [y_{k-1} \ y_{k-2} \ \dots \ y_0].$$

It turns out that imposing this requirement while insisting B_k is a symmetric matrix is, generally speaking, not possible. The need to relax these conditions becomes apparent when one considers that if $B_k S_k = Y_k$ then it follows that $S_k^T B_k S_k = S_k^T Y_k$, giving that if B_k is symmetric then $S_k^T Y_k$ must be symmetric [3]. Unfortunately, $S_k^T Y_k$ is usually not symmetric. Instead of strictly imposing both the multiple secant conditions and symmetry, some of these conditions must be relaxed.

One way to relax these conditions is to ensure the multiple secant conditions hold but not enforce symmetry. In [3], Schnabel generalizes the Powell-Symmetric-Broyden (PSB), Broyden-Fletcher-Goldfarb-Shanno (BFGS), and the Davidon-Fletcher-Powell (DFP) updates to satisfy $B_k S_k = Y_k$. However, in each case, these generalizations may not be symmetric and there are conditions that must be met for the updates to be well-defined. Alternatively, one may relax the multiple secant equations but enforce symmetry. An example of this is found in the same paper when Schnabel proposes perturbing Y_k to obtain a symmetric matrix.

Another type of relaxation takes the form of an approximation of the true $S_k^T Y_k$ using a symmetrization of this matrix. In [1], the following symmetrization is proposed:

$$\text{sym}(A) = \begin{cases} A_{ij}, & i \geq j \\ A_{ji}, & i < j. \end{cases}$$

With this symmetrization, a MSS method (and its limited-memory version described in [2]) is a symmetric method, generating a sequence of symmetric Hessian approximations. (For more details on this symmetrization, see [1, 2].) A crucial aspect of these MSS methods is that they generate a sequence of matrices that are not necessarily positive definite. It is for this reason that these methods are incorporated into trust-region methods. The update formula found in [1, 2] is a rank-2 update formula. As with traditional quasi-Newton methods, in order to maintain the low-memory advantages of limited-memory versions of the methods, a scalar multiple of the identity matrix is used to initialize the sequence of matrices. (For the duration of the paper, this initialization will be referred to as a “one-parameter initialization,” with the parameter being chosen as a scalar.) It is worth noting that it is possible to use general diagonal matrices as an initialization and maintain the low-memory advantage; however, constant diagonal initializations are the most popular approach due to their ease of use.

In this paper, we propose using a *compact formulation* for the sequence of matrices produced by the MSS method found in [1, 2] to allow the use of two parameters to define the initial approximate Hessian. This initialization exploits the form of the compact formulation to create a dense initialization when the two parameters are different. (It is worth noting that when the two parameters are chosen to be the same, the initialization simplifies to the traditional one-parameter initialization.) This work is inspired by the positive results found using a two-parameter initialization for the BFGS update [4]. We demonstrate that the eigenspace associated with all the eigenvalues is unchanged using two parameters in lieu of the usual single parameter. Additionally, some motivation for good choices of initial parameters are presented.

This paper is organized in five sections. In Section 2, we review the compact formulation for the limited-memory MSS matrix. In Section 3, we derive the proposed limited-memory MSS method. This proposed method is incorporated into a traditional trust-region method in Section 4. Numerical comparisons with the MSS method using traditional initializations on large unconstrained problems from the CUTEst test collection [5] are given in Section 5. Finally, Section 6 includes some concluding remarks and observations.

1.1. Notation and Glossary. Unless explicitly indicated, $\|\cdot\|$ denotes the Euclidean two-norm or its subordinate matrix norm. The symbol e_i denotes the i^{th} canonical basis vector whose dimension depends on context.

1.2. Dedication. The idea to use a dense initialization for the MSS method is due to Oleg Burdakov. An initial conversation with him about this work occurred in early 2021 and several follow-up emails were exchanged. Unfortunately, Oleg passed away before the first draft of this paper was written. We dedicate this paper to him.

2. BACKGROUND

In this section, we review how MSS matrices have been constructed, their compact formulation, and a brief overview of how they can be used in MSS methods for unconstrained optimization.

2.1. MSS matrices. Given a sequence of iterates $\{x_i\}$, we define

$$S_k = [s_{k-1} \ s_{k-2} \ \dots \ s_0] \quad \text{and} \quad Y_k = [y_{k-1} \ y_{k-2} \ \dots \ y_0], \quad (2)$$

where $s_i \triangleq x_{i+1} - x_i$ and $y_i \triangleq \nabla f(x_{i+1}) - \nabla f(x_i)$ for $i = 0, \dots, k$. For simplicity we assume S_k has full column rank. (The case when it does not have full column rank is discussed in Section 5.) The multiple secant conditions used to define a multipoint symmetric secant method are

$$B_k S_k = Y_k. \quad (3)$$

As noted in the introduction both symmetry and the multiple secant conditions cannot usually be enforced. In this work, the multiple secant conditions are relaxed by applying the symmetrization transformation [1, 2]:

$$\text{sym}(A) = \begin{cases} A_{ij} & \text{if } i \geq j, \\ A_{ji} & \text{if } i < j, \end{cases} \quad (4)$$

to $S_k^T Y_k$ to guarantee symmetry. Suppose we write

$$S_k^T Y_k = L_k + E_k + T_k, \quad (5)$$

where L_k is the strictly lower triangular, E_k is the diagonal, and T_k is the strictly upper triangular part of $S_k^T Y_k$. With this notation, $\text{sym}(S_k^T Y_k) = L_k + E_k + L_k^T$. It can be shown that the MSS matrix B_k satisfies

$$S_k^T B_k S_k = \text{sym}(S_k^T Y_k), \quad (6)$$

for all $0 < k \leq n$ (see [6]).

With this relaxation, the recursion formula to generate MSS matrices is a rank-2 formula given by

$$B_{k+1} = B_k + \frac{(y_k - B_k s_k) c_k^T + c_k (y_k - B_k s_k)^T}{s_k^T c_k} - \frac{(y_k - B_k s_k)^T s_k c_k c_k^T}{(s_k^T c_k)^2}, \quad (7)$$

where $c_k \in \mathfrak{R}^n$ is any vector such that $c_k^T s_i = 0$ for all $0 \leq i < k$ and $c_k^T s_k \neq 0$ [1]. Interestingly, if c is replaced by αc for any $\alpha \neq 0$, B_{k+1} in (7) does not change [1]. Thus, B_{k+1} is invariant with respect to the scaling of c . The recursion relation (7), absent the additional orthogonality requirements on c_k , is a well-known recursion [7] that can be used to derive the Powell symmetric Broyden (PSB) and the Davidon-Fletcher-Powell (DFP) update. Specifically, when $c_k = s_k$ or $c_k = y_k$, the updates are exactly the PSB and DFP update, respectively. Similar to the PSB update, the MSS update can yield indefinite matrices.

The choice of the vectors $\{c_k\}$ are not unique, and thus, the sequence $\{B_k\}$ is not unique. In [2, 6], the following choice is made for c_k so that $\{B_k\}$ satisfies a least-change problem:

$$c_k \triangleq \left[I - S_k (S_k^T S_k)^{-1} S_k^T \right] s_k.$$

For the duration of this paper, we assume this choice for $\{c_k\}$. For more details, see [1, 2]. In the following lemma, we show that despite the relaxation, the original secant condition is still satisfied.

Lemma 1. *MSS matrices satisfy the secant condition $B_{k+1} s_k = y_k$.*

Proof. Lemma 1 The proof makes use of the rank-2 formula (7):

$$\begin{aligned} B_{k+1} s_k &= \left[B_k + \frac{(y_k - B_k s_k) c_k^T + c_k (y_k - B_k s_k)^T}{s_k^T c_k} - \frac{(y_k - B_k s_k)^T s_k c_k c_k^T}{(s_k^T c_k)^2} \right] s_k \\ &= B_k s_k + \frac{(y_k - B_k s_k) c_k^T s_k + c_k (y_k - B_k s_k)^T s_k}{s_k^T c_k} - \frac{(y_k - B_k s_k)^T s_k c_k c_k^T s_k}{(s_k^T c_k)^2} \\ &= B_k s_k + (y_k - B_k s_k) + \frac{c_k (y_k - B_k s_k)^T s_k}{s_k^T c_k} - \frac{(y_k - B_k s_k)^T s_k c_k}{(s_k^T c_k)} \\ &= y_k. \end{aligned}$$

□

2.2. Compact formulation and the limited-memory case. Given an initial B_0 , Brust [6] derives the compact formulation $B_k = B_0 + \Psi_k M_k \Psi_k^T$, where

$$\Psi_k \triangleq \begin{bmatrix} S_k & (Y_k - B_0 S_k) \end{bmatrix} \quad \text{and} \quad M_k \triangleq \begin{bmatrix} W(S_k^T B_0 S_k - (T_k + E_k + T_k^T))W & W \\ W & 0 \end{bmatrix}, \quad (8)$$

$W \triangleq (S_k^T S_k)^{-1}$, and L_k , E_k , and T_k are defined as in (5). It is worth noting that $B_0 S_k$ in (8) is not difficult to compute when B_0 is the dense matrix proposed in this paper (see Section 5 for details).

Limited-memory MSS matrices are obtained by storing no more than m of the most recently-computed quasi-Newton pairs. As in typical limited-memory quasi-Newton methods, m is typically less than 10 (e.g., Byrd et al. [8] suggest $m \in [3, 7]$). In the limited-memory case, the compact formulation given in (8) holds but with S_k and Y_k defined to contain at most m vectors where $m \ll n$, i.e.,

$$S_k = [s_{k-1} \ s_{k-2} \ \dots \ s_{k-l}] \in \mathfrak{R}^{n \times l} \quad \text{and} \quad Y_k = [y_{k-1} \ y_{k-2} \ \dots \ y_{k-l}] \in \mathfrak{R}^{n \times l}, \quad (9)$$

where $l \leq m$. In the compact representation (8), M_k is at most size $2m \times 2m$, making it a small enough matrix to perform linear algebra operations that are ill-suited for larger (e.g., $n \times n$) matrices. For the duration of the paper, we assume the MSS method is the limited-memory version where S_k and Y_k are defined by (9).

2.3. MSS methods. The MSS matrices used in this work have been proposed to solve systems of equations [1], bound constrained optimization problems [2], and unconstrained optimization [6] problems. In this section, we review how they can be used to solve (1). Because MSS matrices can be indefinite, it is natural to use this sequence of matrices as approximations to the true Hessian in a trust-region method for solving nonconvex optimization problems. We briefly review trust-region methods here, but further details can be found in standard optimization textbooks (see, e.g., [9]).

At each iterate, trust-region methods use a quadratic approximation m_k to model f at the current iterate in a small region neighborhood about the current iterate x_k :

$$m_k(x_k + s) = f(x_k) + g_k^T s + \frac{1}{2} s^T B_k s, \quad (10)$$

where $g_k = \nabla f(x_k)$ and $B_k \approx \nabla^2 f(x_k)$. At each iteration, trust-region methods solve the so-called *trust-region subproblem* to obtain a new search direction $s_k \in \mathfrak{R}^n$:

$$s_k = \arg \min_{\|s\| \leq \Delta_k} g_k^T s + \frac{1}{2} s^T B_k s, \quad (11)$$

where Δ_k is the trust-region radius, and $\|\cdot\|$ is any vector norm. Notice that the difference between the quadratic function in (11) and the model function (10) is a constant, which does not affect the solution of the subproblem. Having obtained a search direction s_k , a basic trust-region algorithm computes a new iterate $x_{k+1} = x_k + s_k$, provided s_k satisfies a sufficient decrease criteria. (For more details, see, e.g., [9, 10].)

One of the advantages of using the Euclidean norm to define the trust region is that the subproblem is guaranteed to have an optimal solution. The following theorem [11, 12] classifies a global solution to the trust-region subproblem defined using the Euclidean norm:

Theorem 1. *Let Δ be a positive constant. A vector s^* is a global solution of the trust-region subproblem (11) where $\|\cdot\|$ is the Euclidean norm if and only if $\|s^*\| \leq \Delta$ and there exists a unique $\sigma^* \geq 0$ such that $B + \sigma^* I$ is positive semidefinite and*

$$(B + \sigma^* I)s^* = -g \quad \text{and} \quad \sigma^*(\Delta - \|s^*\|_2) = 0. \quad (12)$$

Moreover, if $B + \sigma^ I$ is positive definite, then the global minimizer is unique.*

It should be noted that these optimality conditions also serve as the basis for some algorithms to find the solution to subproblems defined by the Euclidean norm. Specifically, these algorithms find an optimal solution by searching for a point that satisfies the conditions given in (12) (see, e.g., [12, 13, 14, 15].)

The MSS method proposed in this paper uses a trust-region method defined by the Euclidean norm. The method solves each trust-region subproblem using the ideas in [15] for solving indefinite subproblems. The following section overviews these ideas.

2.4. The Orthonormal basis L-SR1 (OBS) method. The OBS method [15] is a trust-region method for solving limited-memory symmetric rank-one (L-SR1) trust-region subproblems. The method is able to solve subproblems to high accuracy by exploiting the optimality conditions given in Theorem 1. L-SR1 matrices are generated by a recursion relation using rank-1 updates that satisfy the secant

condition $B_{k+1}s_k = y_k$ for all k . Importantly, as with MSS matrices, L-SR1 matrices can be indefinite. (For details on L-SR1 matrices and methods see, e.g., [9].)

The OBS method makes use of the partial spectral decomposition that can be computed efficiently from the compact formulation [14, 15, 16]. In particular, suppose the compact formulation of an L-SR1 matrix B_{k+1} is given by $B_{k+1} = B_0 + \Psi M \Psi^T$, with $B_0 = \gamma I$. Further, suppose $\Psi = QR$ is the “thin” QR factorization of Ψ where $Q \in \mathfrak{R}^{n \times (k+1)}$ and $R \in \mathfrak{R}^{(k+1) \times (k+1)}$ is invertible. Then,

$$B_{k+1} = \gamma I + QRM R^T Q^T,$$

where $RM R^T$ is a small $(k+1) \times (k+1)$ matrix (i.e., the number of stored quasi-Newton pairs is $k+1$.) Given the spectral decomposition $U \hat{\Lambda} U^T$ of $RM R^T$, the spectral decomposition of B_{k+1} can be written as $B_{k+1} = P \Lambda P^T$, where

$$\Lambda \triangleq \begin{bmatrix} \hat{\Lambda} + \gamma I & 0 \\ 0 & \gamma I \end{bmatrix} \quad \text{and} \quad P \triangleq [QU \quad (QU)^\perp].$$

For more details on this derivation for the L-SR1 case, see [15].

The OBS method uses the above derivation to determine the eigenvalues of B_k at each iteration. Then, depending on the definiteness of B_k , the method computes a high-accuracy solution using the optimality conditions. In some cases, a global solution can be computed directly by formula; in other cases, Newton’s method must be used to compute σ^* and then p^* is computed directly by solving $(B + \sigma I)p^* = -g$. It is worth noting that in the latter case, Newton’s method can be initialized to guarantee that Newton converges monotonically without needing any safeguarding. Moreover, a high-accuracy solution can also be computed in the so-called *hard case* [15].

The OBS method can be generalized to solve trust-region subproblems where the approximation to the Hessian admits any compact representation. The addition of a second parameter to the compact formulation (e.g., the proposed dense initialization) requires significant modifications to the code. However, the resulting code makes use of the same strategy as the OBS method. The partial spectral decomposition of a MSS matrix is carefully presented in the following section.

3. THE DENSE INITIALIZATION

In this section, we propose a MSS method with a dense initialization. In order to introduce the dense initialization, we begin by demonstrating how to compute a partial spectral decomposition of an MSS matrix in order to lay the groundwork for the dense initialization.

3.1. The spectral decomposition. Recall the compact formulation of a MSS matrix:

$$B_k = B_0 + \Psi_k M_k \Psi_k^T, \tag{13}$$

where

$$\Psi_k \triangleq [S_k \quad (Y_k - B_0 S_k)] \quad \text{and} \quad M_k \triangleq \begin{bmatrix} W(S_k^T B_0 S_k - (T_k + E_k + T_k^T))W & W \\ W & 0 \end{bmatrix}, \tag{14}$$

$W \triangleq (S_k^T S_k)^{-1}$, and L_k , E_k , and T_k are defined as in (5). Note that this factorization does not require B_0 to be a scalar multiple of the identity matrix. We assume that $\Psi_k \in \mathfrak{R}^{n \times 2l}$ and $M_k \in \mathfrak{R}^{2l \times 2l}$ where $l \leq m$, and m is the maximum number of stored quasi-Newton pairs.

For this derivation of the partial spectral decomposition of B_k , we assume $B_0 = \gamma_k I$ for simplicity. If the “thin” QR factorization of Ψ_k is $\Psi_k = QR$, where $Q \in \mathfrak{R}^{n \times 2l}$ and $R \in \mathfrak{R}^{2l \times 2l}$ then

$$B_k = B_0 + QRM_kR^TQ^T.$$

The matrix $RM_kR^T \in \mathfrak{R}^{2l \times 2l}$ is small, and thus, its spectral decomposition can be computed in practice. Let $U\hat{\Lambda}U^T$ be the spectral decomposition of $RM_kR^T \in \mathfrak{R}^{2l \times 2l}$. This gives us

$$B_k = B_0 + QU\hat{\Lambda}U^TQ^T, \quad (15)$$

and so, $B_k = P\Lambda P^T$ where

$$\Lambda \triangleq \begin{bmatrix} \hat{\Lambda} + \gamma_k I & 0 \\ 0 & \gamma_k I \end{bmatrix} \quad \text{and} \quad P \triangleq [QU \quad (QU)^\perp]. \quad (16)$$

Here, Λ is a diagonal matrix whose first $2l$ entries are $\hat{\lambda}_i + \gamma_k$, where $\hat{\Lambda} = \text{diag}(\hat{\lambda}_1, \dots, \hat{\lambda}_{2l})$, and the $(2,2)$ -block of Λ contains the eigenvalue γ_k with multiplicity $n - 2l$. The first $2l$ columns of P are made up of QU , which is orthogonal since it is the product of two orthogonal matrices. In contrast, $(QU)^\perp \in \mathfrak{R}^{n \times (n-2l)}$ is very computationally expensive to compute and will never be explicitly used. Finally, provided Ψ_k has full column rank, it is worth noting that it is possible to form QU without storing Q ; namely, QU can be computed using the formula $QU = \Psi_k R^{-1}U$. For simplicity, we define $P_\parallel = QU$ so that $P = [P_\parallel \quad P_\perp]$, where $P_\perp = P_\parallel^\perp$. Notice that this is the same form as the spectral decomposition in (16) but with different-sized matrices.

3.2. The dense initial matrix. In the previous subsection, we assumed that $B_0 = \gamma_k I$, i.e., a scalar multiple of the identity matrix. In this subsection, we show how the spectral decomposition of B_k can be used to design a two-parameter dense initialization.

Consider the spectral decomposition $B_k = P\Lambda P^T$ where Λ and P are defined in (16). In the case that $B_0 = \gamma_k I$, then $B_0 = \gamma_k P P^T$ since P is orthogonal. Moreover, B_0 can be written as

$$B_0 = \gamma_k P_\parallel P_\parallel^T + \gamma_k P_\perp P_\perp^T.$$

The dense initialization is formed by assigning a different parameter to each subspace, i.e.,

$$\tilde{B}_0 = \zeta_k P_\parallel P_\parallel^T + \zeta_k^C P_\perp P_\perp^T, \quad (17)$$

where ζ_k and ζ_k^C can be updated each iteration.

Theorem 2. *Given \tilde{B}_0 as in (17), then B_k in (13) has the following spectral decomposition:*

$$B_k = [P_\parallel \quad P_\perp] \begin{bmatrix} \hat{\Lambda} + \zeta_k I & 0 \\ 0 & \zeta_k^C I \end{bmatrix} \begin{bmatrix} P_\parallel^T \\ P_\perp^T \end{bmatrix}. \quad (18)$$

Proof. By (15) and (17), we have

$$\begin{aligned} B_k &= \tilde{B}_0 + \Psi_k M_k \Psi_k^T \\ &= \tilde{B}_0 + P_\parallel \hat{\Lambda} P_\parallel^T \\ &= \zeta_k P_\parallel P_\parallel^T + \zeta_k^C P_\perp P_\perp^T + P_\parallel \hat{\Lambda} P_\parallel^T \\ &= [P_\parallel \quad P_\perp] \begin{bmatrix} \hat{\Lambda} + \zeta_k I & 0 \\ 0 & \zeta_k^C I \end{bmatrix} \begin{bmatrix} P_\parallel^T \\ P_\perp^T \end{bmatrix}. \end{aligned}$$

□

Corollary 1. *The eigenspace associated with the eigenvalues of B_k is not changed using the dense initialization (17) in lieu of the one-parameter initialization.*

3.3. Parameter choices. One possible motivation to pick ζ_k is to better ensure that the multiple secant conditions hold, i.e., $B_k S_k = Y_k$ for all k . Thus, ζ_k can be selected to be the solution of the following minimization problems:

$$\tilde{B}_0 = \arg \min_{\tilde{B}_0} \|B_0 S_k - Y_k\|_F^2 \quad \text{or} \quad \tilde{B}_0 = \arg \min_{\tilde{B}_0} \|B_0^{-1} Y_k - S_k\|_F^2, \quad (19)$$

where $\|\cdot\|_F$ denotes the Frobenius norm.

The following two lemmas and their corollaries are useful for solving both minimization problems in (19).

Lemma 2. *The following relationships hold between S_k , Ψ_k and P_{\parallel} : (i) $\text{Range}(S_k) \subseteq \text{Range}(\Psi_k)$, (ii) $\text{Range}(S_k) \subseteq \text{Range}(P_{\parallel})$, and (iii) $P_{\parallel} P_{\parallel}^T S_k = S_k$.*

Proof. Since $\Psi_k = [S_k \ Y_k - B_0 S_k]$ it follows immediately that $\text{Range}(S_k) \subseteq \text{Range}(\Psi_k)$. Note that $P_{\parallel} = \Psi_k R^{-1} U$, it follows that $\text{Range}(\Psi_k) = \text{Range}(P_{\parallel})$. Finally, $P_{\parallel} P_{\parallel}^T S_k = S_k$ since $\text{Range}(S_k) \subseteq \text{Range}(P_{\parallel})$. □

Corollary 2. *Suppose \tilde{B}_0 is as in (17). Then, $\tilde{B}_0 S_k = \zeta_k S_k$.*

Proof. By Lemma 2,

$$\tilde{B}_0 S_k = (\zeta_k P_{\parallel} P_{\parallel}^T + \zeta_k^C P_{\perp} P_{\perp}^T) S_k = \zeta_k P_{\parallel} P_{\parallel}^T S_k = \zeta_k S_k.$$

□

Lemma 3. *The following relationships hold between Y_k , Ψ_k and P_{\parallel} : (i) $\text{Range}(Y_k) \subseteq \text{Range}(\Psi_k)$, (ii) $\text{Range}(Y_k) \subseteq \text{Range}(P_{\parallel})$, and (iii) $P_{\parallel} P_{\parallel}^T Y_k = Y_k$.*

Proof. To show (i), we prove that Y_k can be written as a linear combination of the columns of Ψ_k . Namely, by Corollary 2,

$$Y_k = \zeta_k S_k + (Y_k - \tilde{B}_0 S_k) = [S_k \ Y_k - \tilde{B}_0 S_k] \begin{bmatrix} \zeta_k I \\ I \end{bmatrix} = \Psi_k \begin{bmatrix} \zeta_k I \\ I \end{bmatrix}.$$

Since $P_{\parallel} = \Psi_k R^{-1} U$, it follows that $\text{Range}(Y_k) \subseteq \text{Range}(P_{\parallel})$, giving (ii). Finally, $P_{\parallel} P_{\parallel}^T Y_k = Y_k$ since $\text{Range}(Y_k) \subseteq \text{Range}(P_{\parallel})$. □

Corollary 3. *Suppose \tilde{B}_0 is as in (17). Then, $\tilde{B}_0^{-1} S_k = (1/\zeta_k) S_k$.*

Proof. By Lemma 3,

$$\tilde{B}_0^{-1} Y_k = \left(\frac{1}{\zeta_k} P_{\parallel} P_{\parallel}^T + \frac{1}{\zeta_k^C} P_{\perp} P_{\perp}^T \right) Y_k = \frac{1}{\zeta_k} P_{\parallel} P_{\parallel}^T Y_k = \frac{1}{\zeta_k} Y_k.$$

□

The optimal values for ζ_k that solve (19) are given in the following theorem.

Theorem 3. *If \tilde{B}_0 is chosen to be in the form of (17), the solutions to*

$$\hat{B}_0 \triangleq \arg \min_{\tilde{B}_0} \left\| \tilde{B}_0 S_k - Y_k \right\|_F^2 \quad \text{and} \quad \bar{B}_0 \triangleq \arg \min_{\tilde{B}_0} \left\| \tilde{B}_0^{-1} Y_k - S_k \right\|_F^2$$

are, respectively, $\hat{B}_0 = \hat{\zeta}_k P_{\parallel} P_{\parallel}^T + \hat{\zeta}_k^C P_{\perp} P_{\perp}^T$ and $\bar{B}_0 = \bar{\zeta}_k P_{\parallel} P_{\parallel}^T + \bar{\zeta}_k^C P_{\perp} P_{\perp}^T$, where

$$\hat{\zeta}_k = \frac{\text{trace}(S_k^T Y_k)}{\text{trace}(S_k^T S_k)} \quad \text{and} \quad \bar{\zeta}_k = \frac{\text{trace}(Y_k^T Y_k)}{\text{trace}(S_k^T Y_k)}, \quad (20)$$

and $\hat{\zeta}_k, \bar{\zeta}_k \in \Re$.

Proof. Consider the problem

$$\hat{B}_0 \triangleq \arg \min_{\tilde{B}_0} \left\| \tilde{B}_0 S_k - Y_k \right\|_F^2,$$

which can be restated as finding $\hat{\zeta}_k$ and $\hat{\zeta}_k^C$ that solve the following optimization problem:

$$\arg \min_{\hat{\zeta}_k, \hat{\zeta}_k^C} \left\| \left(\hat{\zeta}_k P_{\parallel} P_{\parallel}^T + \hat{\zeta}_k^C P_{\perp} P_{\perp}^T \right) S_k - Y_k \right\|_F^2. \quad (21)$$

By Lemma 2, the problem (21) is equivalent to

$$\arg \min_{\hat{\zeta}_k} \left\| \hat{\zeta}_k S_k - Y_k \right\|_F^2,$$

which can be written as follows:

$$\arg \min_{\hat{\zeta}_k} \left\{ \text{trace} \left(\left(\hat{\zeta}_k S_k - Y_k \right)^T \left(\hat{\zeta}_k S_k - Y_k \right) \right) \right\}. \quad (22)$$

The minimization problem (22) is a one-dimensional optimization problem in $\hat{\zeta}_k$ that can be solved by differentiating the objective function in (22) with respect to $\hat{\zeta}_k$ and setting the result to zero:

$$\frac{d}{d\hat{\zeta}_k} \left[\text{trace}(\hat{\zeta}_k^2 S_k^T S_k - 2\hat{\zeta}_k S_k^T Y_k + Y_k^T Y_k) \right] = 2\hat{\zeta}_k \text{trace}(S_k^T S_k) - 2\text{trace}(S_k^T Y_k) = 0.$$

This yields the following solution:

$$\hat{\zeta}_k = \frac{\text{trace}(S_k^T Y_k)}{\text{trace}(S_k^T S_k)}. \quad (23)$$

Note that $\hat{\zeta}_k$ in (23) is the minimizer since the function to be minimized is both convex and quadratic in $\hat{\zeta}_k$. The solution \bar{B}_0 can be obtained using a similar process. \square

This strategy for choosing the two parameters does not specify $\hat{\zeta}_k^C$; in fact, this parameter is irrelevant to solving the minimization problem. Also, notice that when $k = 1$, $\bar{\zeta}_k$ is the conventional initialization for the BFGS method and sometimes referred to as the Barzilai and Borwein (BB) initialization [17].

It is also worth noting that applying either choice of ζ_k from this theorem could result in a choice of ζ_k that is negative. The disadvantage of negative ζ_k is that the initial B_0 will have $2l$ negative eigenvalues. While rank-2 updates could shift these eigenvalues into positive territory, the subproblem solver will need to be computing solutions on the boundary of the trust region as long as any eigenvalue of B_k is negative. This is undesirable for two reasons (i) at a local solution of (1) it is desirable that B_k is positive definite and (ii) it is more computationally expensive for the subproblem solver to compute solutions on the boundary than in the interior of the trust region.

3.4. **Selecting ζ_k^C .** While the subspace P_{\parallel} is constructed from the pairs of current limited-memory iterates $\{s_i, y_i\}$, $i = k - l, \dots, k - 1$, the subspace P_{\perp} is unknown. In [4], Brust et al. propose suggestions for the second parameter in the proposed dense initialization for an L-BFGS method. These suggestions are based on the trust-region subproblem solver that is applicable in our proposed method. Indeed, the same comments apply to the generalized OBS method found in Section 2.4. There is an inverse relationship between ζ_k^C and the subspace P_{\perp} . Specifically, if ζ_k^C is large then the component of the solution to the trust-region subproblem that lies in the subspace P_{\perp} will be small in norm. See [4] for details. However, choices of ζ_k^C that are too large or too small may lead to poorly-conditioned approximate Hessians. Strategies such as taking ζ_k^C to be convex combinations of the current ζ_k and previous values of ζ_k have been found to be beneficial in the BFGS case [4].

4. THE PROPOSED MSS METHOD

In this section, we present the proposed MSS method. This method uses a trust-region method whose subproblems are defined using a MSS matrix. The result is a type of limited-memory quasi-Newton trust-region method whose approximate Hessian can be indefinite at any given iteration. Finally, this section concludes with a discussion of the computational cost of the proposed method.

4.1. Full rank assumptions.

4.2. **Ensuring S_k has full rank.** In order for the compact formulation to exist, it must be the case that S_k has full rank so that $W = (S_k^T S_k)^{-1}$ in (8) is well-defined. To ensure this, the LDL^T factorization of $S_k^T S_k$ is computed to find linearly dependent columns in S_k . Specifically, small diagonal elements in D correspond to columns of S_k that are linearly dependent. Let \hat{S}_k denote the matrix S_k after removing the linearly dependent columns. The resulting matrix $\hat{W} \triangleq (\hat{S}_k^T \hat{S}_k)^{-1}$ is positive definite, and thus, invertible. This strategy is not new and was first proposed in this context in [14]. For notational simplicity, we assume that S_k has linearly independent columns for the remainder of this section because if it is not full rank, linear dependence will be removed by this procedure. For the proposed MSS method, a full rank S_k is used to define Ψ_k .

4.3. **Ensuring Ψ_k has full rank.** It is also desirable that Ψ_k is full rank to avoid any adverse effects on the condition number of B_k . If Ψ_k is not full rank, then $\hat{\Lambda}$ will have at least one diagonal entry that is close to zero (the number of small diagonal elements of R will correspond to the number of small eigenvalues of $RM R^T$). Without loss of generality, assume that i is such that $\hat{\lambda}_i + \zeta_k \approx \zeta_k$, i.e., $\hat{\lambda}_i \approx 0$. In the cases when $|\hat{\lambda}_i + \zeta_k| \approx |\zeta_k|$ is the largest or smallest approximate eigenvalue of B_k in absolute value, the condition number of B_k will be negatively affected, possibly detrimentally. In contrast, if $|\hat{\lambda}_j + \zeta_k| \leq |\zeta_k| \leq |\hat{\lambda}_{\hat{k}} + \zeta_k|$ for some $j, \hat{k} \in \{0, 1, \dots, 2\text{rank}(S)\}$ then the condition number of B_k will not be impacted. For this reason, ensuring that Ψ has full rank will help prevent unnecessary ill-conditioning.

In order to enforce that Ψ_k has full rank, we also perform the LDL^T factorization of $\Psi_k^T \Psi_k$ to find linearly dependent columns of Ψ_k , similar to the procedure to ensure that S_k is full rank.

4.4. LDL^T and its effect on the eigendecomposition. Using the LDL^T factorization of $\Psi_k^T \Psi_k$ in lieu of the QR factorization of Ψ_k in Section 3.1 requires redefining the eigendecomposition of B_k . The following presentation is based on [18]. For notational simplicity, the subscript k is dropped for all matrices.

Suppose $\Pi^T \Psi^T \Psi \Pi = LDL^T$ is the LDL^T factorization of $\Psi^T \Psi$ and Π is a permutation matrix¹. Let J be the set of indices such that its corresponding diagonal entry in D and that of its “pair” is sufficiently large (see Section 4.7). Then,

$$\Psi^T \Psi \approx \Pi L_{\dagger} D_{\dagger} L_{\dagger}^T \Pi^T = \Pi R_{\dagger}^T R_{\dagger} \Pi^T,$$

where L_{\dagger} is the matrix L having removed columns indexed by an element not in J , D_{\dagger} is the matrix D having removed any rows and columns indexed by an element not in J , $R_{\dagger} \triangleq \sqrt{D_{\dagger}} L_{\dagger}^T \in \mathfrak{R}^{r \times 2l}$, and $r = |J|$. This gives the approximate decomposition of B_k :

$$B_k = B_0 + Q_{\dagger} R_{\dagger} \Pi^T M \Pi R_{\dagger}^T Q_{\dagger}^T, \quad (24)$$

where $Q_{\dagger} \triangleq (\Psi \Pi)_{\dagger} R_{\dagger}^{-1}$, $(\Psi \Pi)_{\dagger}$ is the matrix $\Psi \Pi$ having deleted columns not indexed in J , and R_{\dagger} is R_{\dagger} having removed columns not indexed in J . (For more details on this derivation, see [18].)

The partial eigendecomposition proceeds as in Section 3.1 but with $R_{\dagger} \Pi^T M \Pi R_{\dagger}^T$ in lieu of RMR^T . Finally, as in [18], P_{\parallel} can be computed as

$$P_{\parallel} = (\Psi \Pi)_{\dagger} R_{\dagger}^{-1} U. \quad (25)$$

4.5. The benefits of two LDL^T factorizations. While ensuring Ψ_k is full rank is sufficient to identify the columns of S_k that are linearly independent, there is a disadvantage to computing only the LDL^T factorization of $\Psi_k^T \Psi_k$ in lieu of the LDL^T factorizations of both of $S_k^T S_k$ and $\Psi_k^T \Psi_k$. Namely, using the LDL^T factorization of $\Psi_k^T \Psi_k$ to identify linearly independent columns of S_k has the potential of forcing the loss of more information. To see this, consider what occurs when only one LDL^T factorization is performed. If the factorization of $\Psi_k^T \Psi_k$ leads to removing a column associated with S_k , (e.g., the column s_i), then the corresponding column of Y_k , (i.e., y_i), must also be removed in order that $S_k^T Y_k$ is computable and the dimensions of M are well-defined. Similarly, if the column of $y_i - B_0 s_i$ of Ψ_k needs to be removed, then to maintain dimension agreement in the compact formulation, both s_i and y_i from S_k and Y_k , respectively, must be removed to compute M . In other words, columns of Ψ_k must be removed in pairs. This can lead to deleterious effects when, for example, Ψ_k for a matrix of size $n \times 2l$ and \hat{l} columns are found to be linearly independent corresponding to different subscripts. In this case, since l is typically chosen to be small, potentially few columns of Ψ_k may remain; moreover, in the extreme case when $\hat{l} = l$ then no columns of Ψ_k will be preserved since columns must be removed in pairs unless additional measures are taken.

In contrast, performing two LDL^T factorizations helps mitigate information loss. Namely, if s_i is called upon to be removed due to the LDL^T factorization of $S_k^T S_k$, it is necessary to remove y_i so that $S_k^T Y_k$ can be computed. The remaining columns of S_k and Y_k are used to form Ψ_k (and M). However, if there is further dependency in Ψ_k , after having removed dependent columns in S_k , then (1) only one column needs to be removed at a time (i.e., if the column $y_i - B_0 s_i$ needs to be removed, the column s_i need not be removed from Ψ_k) and (2) M does not need to be further altered. To

¹For the numerical results, MATLAB’s built-in `ldl` command, which uses rook pivoting[19, 20], is used.

see this, consider equation (24), where columns of Ψ_k are removed, R_{\dagger} and R_{\ddagger} are formed, and M remains intact. In other words, there is no additional information loss in M when columns in Ψ_k are found to be linearly dependent after having already removed linearly dependent columns in S_k (the first block of Ψ_k). Thus, performing two LDL^T decompositions removes the requirement that (1) columns from Ψ_k are always removed in pairs and (2) mitigates additional information loss in M .

4.6. MSS algorithm with a dense initial matrix. The following algorithm is the proposed MSS algorithm. Details follow the algorithm. Brackets are used to denote quantities that are stored using more than one variable. (For example, $[Bp] = -g$ means to store $-g$ in the variable name Bp .) In the below algorithm, m denotes the maximum number of stored quasi-Newton pairs and l denotes the current number of stored pairs. The MSS algorithm requires an initial x as well as a way to compute the function f and its gradient g at any point.

PROCEDURE 1: MSS Method with dense initialization

```

1: Input:  $x$ 
2: Pick  $0 \ll \tau < \hat{\tau}$ ;
3: Set  $m \in [3, 7]$  with  $m \in \mathbb{Z}^+$ ,  $\Delta = 1$ ;
4: Set  $f \leftarrow f(x)$  and  $g \leftarrow g(x)$ ;  $l \leftarrow 0$ ;
5:  $p \leftarrow -g$ ; store  $[Bp] = -g$ ;
6: Use an Amijo backtracking line search to find  $\alpha$ ;  $x \leftarrow x + \alpha p$ ;
7: Update  $f \leftarrow f(x)$  and  $g \leftarrow g(x)$ ;
8: Update  $s$  and  $y$ ;  $l \leftarrow 1$ ;
9: Update  $\Delta$  using Algorithm (2);
10: while not converged do
11:   if  $l \leq m$ , then
12:     Add  $s$  to  $S$  and add  $y$  to  $Y$ ;  $l \leftarrow l + 1$ ;
13:   else
14:     Remove oldest pair in  $S$ ,  $Y$ , and corresponding column in  $\Psi$ ;
15:     Add  $s$  to  $S$  and add  $y$  to  $Y$ ;
16:   end if
17:   Compute  $\zeta$  and  $\zeta^C$  (e.g., Section 3.3); Update  $\Psi$ ;
18:   Ensure  $S$  and  $\Psi$  are full rank using Section 4.2; Store  $R_{\dagger}$ ,  $R_{\ddagger}$ ;
19:   Update  $M$ ;
20:   Compute the spectral decomposition  $U\hat{\Lambda}U^T$  of  $R_{\dagger}\Pi^T M\Pi R_{\dagger}^T$ ;
21:    $\Lambda \leftarrow \hat{\Lambda} + \zeta I$ ;
22:    $[p, Bp] = \text{obs}^*(g, \Psi, R_{\ddagger}^{-1}, U, \Lambda, \zeta, \zeta^C, \Delta)$ ;
23:    $x \leftarrow x + p$ ;
24:    $f \leftarrow f(x)$  and  $g \leftarrow g(x)$ ;
25:   Update  $s$  and  $y$ ;
26:   Update  $\Delta$  using Algorithm (2);
27: end while
28: Output:  $x$ 

```

Algorithm 1 begins by letting $B_0 = I$, and thus, the search direction is the steepest descent direction. (Future iterations use the dense initialization.) The update to Δ at each iteration makes use of Algorithm 2, which is a standard way to update the trust-region radius (see, for example, [9]). In Algorithm 2, the variable ρ stores the ratio between the actual change and the predicted change. If this ratio is sufficiently large, then the step is accepted and the trust-region radius is possibly updated. If the ratio is too small, the step is rejected and Δ is decreased. Note that the implicit

update to B_k , i.e., the acceptance of a new quasi-Newton pair (lines 8 and 25 in Algorithm 1), is independent of whether the step is accepted in Algorithm 2.

The LDL^T decomposition is used twice in line 18 in Algorithm 1. Each time, the i th diagonal entry of D is considered to be sufficiently large provided

$$D_{ii} > \text{tol} * \max_j |D_{jj}|,$$

where D_{jj} denotes the j th diagonal entry in D and tol is a small positive number (see Sections 4.2-4.3 for more details). Finally, in line (22), a modified `obs` method (denoted by the asterisk) is used to solve the trust-region subproblem.

PROCEDURE 2: Update the trust-region radius

```

1: Fix:  $0 < \eta_1 < \eta_2 < 1$ ,  $0 < \gamma_1, \gamma_p < 1 < \gamma_2$ ;
2:  $\rho \leftarrow (f_{\text{new}} - f) / (-g^T p - 0.5p^T [Bp], 0)$ ;
3: if  $\rho \geq \eta_1$ , then
4:    $f \leftarrow f_{\text{new}}$ ;  $x \leftarrow x + p$  and  $g \leftarrow \nabla f(x)$ ;
5:   if  $\rho \geq \eta_2$ , then
6:     if  $\|p\| > \gamma_p \Delta$ , then
7:        $\Delta \leftarrow \gamma_2 \Delta$ ;
8:     end if
9:   end if
10: else
11:    $\Delta \leftarrow \gamma_1 \Delta$ ;
12: end if

```

Theorem 4. *Let $f : \mathfrak{R}^n \rightarrow \mathfrak{R}$ be a twice-continuously differentiable and bounded below. Suppose there exists scalars $c_1, c_2 > 0$ such that*

$$\|\nabla^2 f(x)\| \leq c_1 \quad \text{and} \quad \|B_k\| \leq c_2, \quad (26)$$

for all $x \in \mathbb{R}^n$ and for all k . Consider the sequence $\{x_k\}$ generated by Algorithm 1 with $\zeta, \zeta^C \in \mathfrak{R}$. Then,

$$\lim_{k \rightarrow \infty} \|\nabla f(x_k)\| = 0.$$

Proof. Since the OBS method generates high-accuracy solutions to the trust-region subproblem, all the assumptions of Theorem 6.4.6 in [10] are met, proving convergence. \square

4.7. Computational complexity. In this section, we consider the computational cost per iteration of Algorithm (1). The LDL^T factorization of $S_k^T S_k$ and $\Psi_k^T \Psi_k$ are each $\mathcal{O}(l^3)$. Moreover, if the LDL^T factorization is updated each iteration instead of computed from scratch, this cost drops to $\mathcal{O}(l^2)$. The spectral decomposition's dominant cost is at most $\mathcal{O}(l^3) = (l^2/n) \mathcal{O}(nl)$, depending on the rank of Ψ_k . Finally, the `obs` method requires two matrix-vector products with P_{\parallel} , whose dominant cost is $\mathcal{O}(4nl)$ flops to solve each trust-region subproblem. (For comparison, this is the same as the dominant cost of L-BFGS [21].)

5. NUMERICAL EXPERIMENTS

The MSS method was developed to solve large-scale unconstrained nonconvex optimization problems. For this reason, the experiments in this section test the performance of the MSS method on a set of large-scale unconstrained optimization problems from the CUTEest test set [5]. Specifically, for these experiments, we considered all problems from CUTEest test set with $n \geq 1000$ of the classification

"OUR2"², which includes all problems with an objective function that is nonconstant, nonlinear, nonquadratic, and not the sum of squares. This selection yielded 60 problems. There were 11 problems on which no method converged and these were removed from the test set resulting in a total of 49 problems on which results are presented.

For these experiments, the trust region was defined using the Euclidean norm, and Algorithms 1-2 were run with the following parameters: $\eta_1 = 0.01$, $\eta_2 = 0.75$, $\gamma_1 = 0.5$, $\gamma_2 = 2$, and $\gamma_p = 0.8$.

In our experiments, we found that updating s and y only when

$$s_i^T y_i > \epsilon \|s_i\| \|y_i\|, \quad (27)$$

where ϵ is machine precision, slightly outperformed the strategies of updating s and y regardless of the sign and magnitude of their inner product. Thus, for all experiments reported in this section, we updated the pairs (s, y) only when they satisfied (27).

For these experiments, the algorithms terminated successfully if iterate x_k satisfied

$$\|g(x_k)\| \leq \max(\tau_g * \|g_0\|, \tau_g),$$

where $\tau_g = 1e^{-5}$ and $g_0 = g(x_0)$. On the other hand, the methods terminated unsuccessfully if either of the following occurred: the number of iterations reached $2n$, the number of function evaluations reached $100n$, or Δ became smaller than 100ϵ , where ϵ denotes machine precision.

The results of experiments are partially summarized using performance profiles, proposed by Dolan and Moré[22]. Specifically, if \mathcal{P} denotes the set of test problems, the performance profiles plot the function $\pi_s : [0, r_M] \rightarrow \mathfrak{R}^+$ defined by

$$\pi_s(\tau) = \frac{1}{|\mathcal{P}|} |\{p \in \mathcal{P} : \log_2(r_{p,s}) \leq \tau\}|,$$

where $r_{p,s}$ denotes the ratio of the number of function evaluations needed to solve problem p with method s with the least number of function evaluations needed to solve p by any method. Note that r_M is the maximum value of $\log_2(r_{p,s})$.

Experiment 1. The first experiment compares the number of function evaluations needed to solve each problem using five different options for initializations (17) found in Table 2. Three memory size limits ($m = 3, 5$, and 7) were tested.

The first initialization option tested is the Barzilai and Borwein (BB) initialization, which is a standard choice for many quasi-Newton methods [17]. This is a one-parameter initialization that does not use a dense initialization; however, we found that this is a very competitive initialization for the MSS method. The second and third options are one-parameter initialization that pick ζ_k based on Theorem 3. The fourth option is a two-parameter initialization that ζ_k to be the maximum ratio of $y_i^T y_i / y_i^T s_i$ where i ranges over the stored updates, and ζ_k^C is chosen as the BB initialization. This initialization is based on ideas in [18]. Finally, the last option can be viewed as a variant of Option 4. In all experiments, safeguarding was use to ensure that ζ_k and ζ_k^C were neither too large nor too small. Specifically, for these

²See <https://www.cuter.rl.ac.uk/Problems/mastsif.shtml> for further classification information.

TABLE 1. Values for different ζ_k and ζ_k^C used in Experiment 1.

	ζ_k	ζ_k^C
Option 1	$\frac{y_k^T y_k}{y_k^T s_k}$	$\frac{y_k^T y_k}{y_k^T s_k}$
Option 2	$\frac{\text{trace}(Y_k^T Y_k)}{\text{trace}(S_k^T Y_k)}$	$\frac{\text{trace}(Y_k^T Y_k)}{\text{trace}(S_k^T Y_k)}$
Option 3	$\frac{\text{trace}(S_k^T Y_k)}{\text{trace}(S_k^T S_k)}$	$\frac{\text{trace}(S_k^T Y_k)}{\text{trace}(S_k^T S_k)}$
Option 4	$\max_{k-1 \leq i \leq k-l} \left\{ \frac{y_i^T y_i}{y_i^T s_i} \right\}$	$\frac{y_k^T y_k}{y_k^T s_k}$
Option 5	$\max_{k-1 \leq i \leq k-l} \left\{ \frac{y_i^T y_i}{y_i^T s_i} \right\}$	$\text{mean}_{k-1 \leq i \leq k-l} \left\{ \frac{y_i^T y_i}{y_i^T s_i} \right\}$

experiments, either parameter was set to its previous value if it fell outside the range $[10^{-4}, 10^4]$. In addition to preventing a parameter from becoming too large, this also prevents either parameter becoming negative leading to indefinite trust-region subproblems (see the discussion at the end of Section 3.2). Finally, for the initial iteration, $\zeta_0 = \zeta_0^C = 1$. The parameters chosen in Table 2 represent some of the best choices that we have found.

For all initializations, $m = 3$ yielded the best results for MSS. Moreover, Options 1, 4, and 5 were the best choices with $m = 3$. Figure 1 displays these results. From the performance profile, it appears that Option 4 outperforms the other two options, including usual quasi-Newton initialization (Option 1). It is important to note that the MSS method performs the same number of function as gradient evaluations (i.e., one per iteration), and thus, the performance profile for gradient evaluations is identical to the one presented for function evaluations.

Table 2 presents the cumulative results for $m = 3$ for all five initializations. In this table, the total number of function evaluations reported includes only the 46 problems on which the MSS method converged using all five initializations. Table 2 shows that Option 4 appears to outperform the other initializations in number of problems MSS could solve but also in terms of the total number of function evaluations when considering only the problems in which all initializations led to convergence for MSS.

TABLE 2. Cumulative results on 49 CUTEst problems for $m = 3$.

	Option 1	Option 2	Option 3	Option 4	Option 5
Problems solved	47	48	48	49	48
Function evaluations (FE)	8295	7570	9255	6809	6944

Finally, for comparison between the different memory allocations, we report in Table 3 the performance of Option 4 using all three memory size $m = 3, 5,$ and 7 . The number of function evaluations found in Table 3 for $m = 3$ are different than in Table 2 since Table 2 reports results only on 46 problems; in contrast, function evaluations for all 49 problems are included in Table 3 since using MSS converged on all 49 problems for all three memory sizes using Option 4.

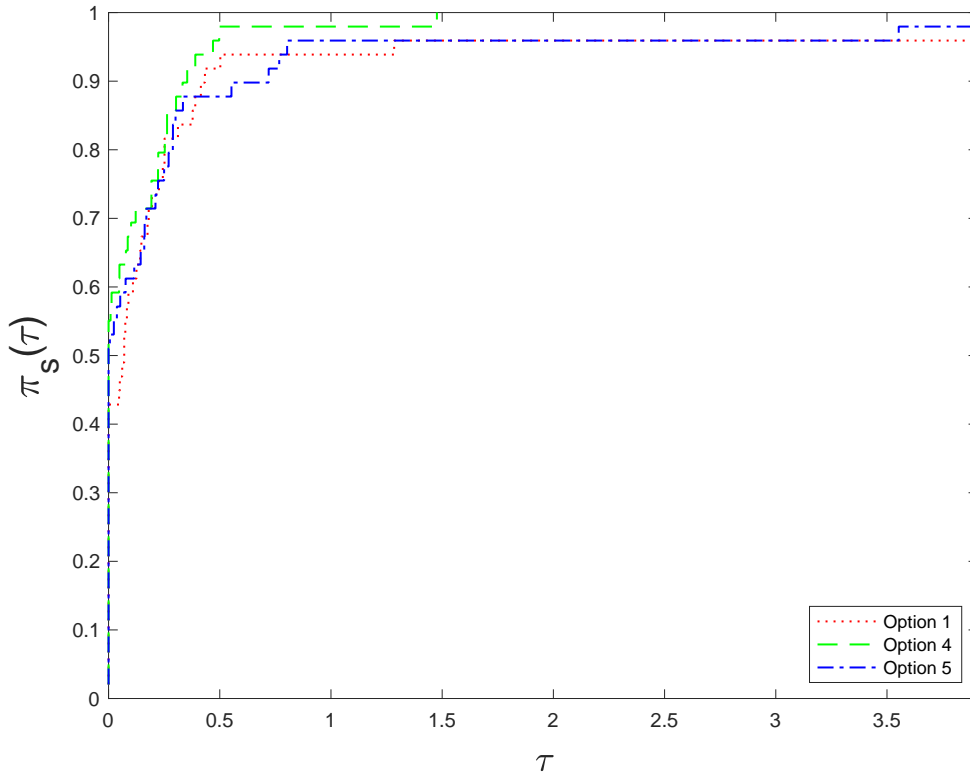


FIGURE 1. Performance profile comparing function evaluations using MSS with three different initializations and $m = 3$.

TABLE 3. Cumulative results on 49 CUTEst problems using MSS with Option 4.

memory	$m = 3$	$m = 5$	$m = 7$
Problems solved	49	49	49
Function evaluations (FE)	12,457	14,613	15,232

Experiment 2. One of the most-used indefinite updates for large-scale optimization is the limited-memory symmetric rank-one (L-SR1). For this experiment, we implemented a standard L-SR1 trust-region method [9, Algorithm 6.2] and chose the approximate solution to the subproblem using a truncated-CG (see, for example, [9, 10]). The LSR-1 method was initialized using $B_0 = \gamma_k^{SR1} I$, where γ_k^{SR1} could be changed each iteration. Updates to the quasi-Newton pairs were accepted provided

$$|s_k^T(y_k - B_k s_k)| \geq \tau_s \|y_k - B_k s_k\| \|s_k\|, \quad (28)$$

where $\tau_s = 1e^{-8}$. For these experiments, the initial iteration used $B_0 = I$, and for subsequent iterations, the LSR-1 method was initialized two standard ways: (1) using the BB initialization and (2) using $B_0 = I$ for every initialization. Since we require (28) to update the pairs, there was no danger of the denominator for the BB initialization becoming zero. For these results, the trust-region framework (e.g., parameters) for the MSS and L-SR1 methods were identical. The results of this experiment are presented in a performance profile and table.

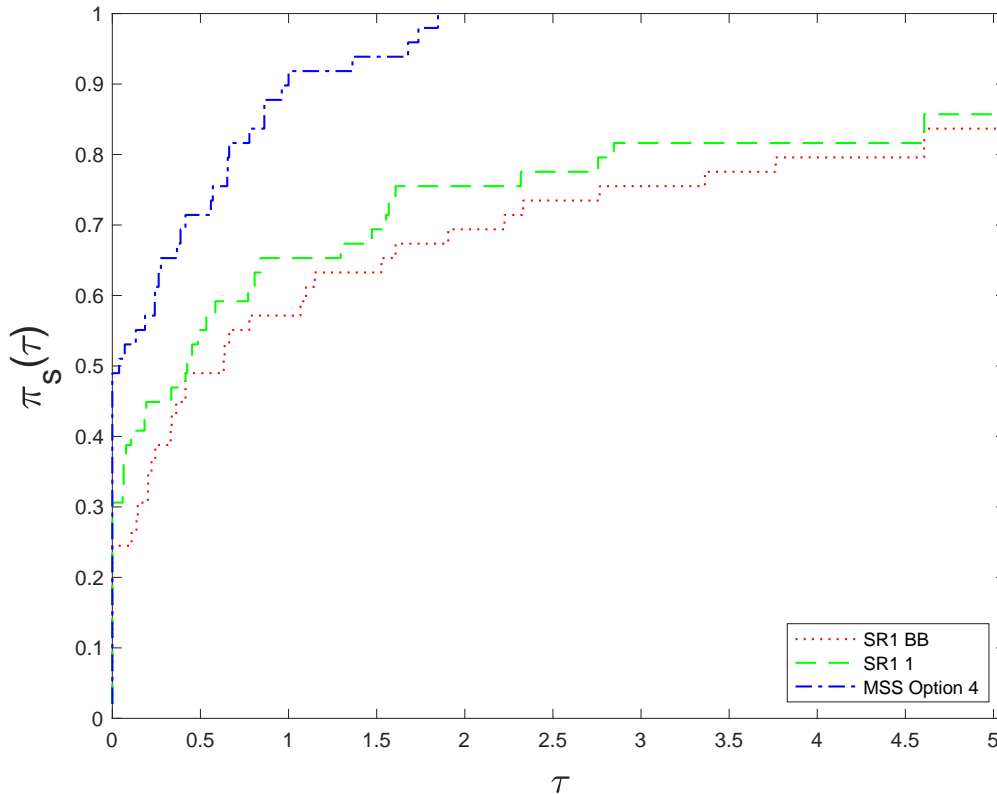


FIGURE 2. Performance profile comparing function evaluations using L-SR1 and MSS with $m = 3$. "SR1 BB" refers to using L-SR1 together with the BB initialization and "SR1 1" refers to using L-SR1 together with the initialization $B_0 = I$ each iteration.

Figure 2 contains the performance profile for function evaluations. From the figure, it appears that MSS with Option 4 outperforms both implementations of L-SR1 in terms of function evaluations using $m = 3$. Table 4 contains cumulative results for $m = 3$ for MSS and the two L-SR1 methods. Of the 49 problems that at least one method converged on, MSS converged on all 49; meanwhile, the L-SR1 methods converged on 41 and 42 depending on the initialization. There were a total of 40 problems in which all three methods converged; the total number of function evaluations on these 40 problems are reported in the last line of table. On the problems in which all three methods converged, MSS required significantly fewer function evaluations. In table 5, the number of problems solved and the number of function evaluations are reported for memory sizes $m = 3$, $m = 5$ and $m = 7$. In all cases, MSS outperformed L-SR1. Note that the total number of function evaluations only counts the 38 problems on which all methods converged using all three memory sizes.

TABLE 4. Cumulative results on 49 CUTEst problems using MSS with Option 4 and L-SR1.

	MSS	L-SR1 BB	L-SR1 1
Problems solved	49	41	42
Function evaluations (FE)	3,120	14,621	11,817

TABLE 5. Cumulative results on 49 CUTEst problems using MSS with Option 4 and L-SR1 for various memory sizes.

Memory	Solver	Problems solved	Function evaluations (FE)
$m = 3$	MSS Option 4	49	2,914
	L-SR1 BB	41	14,142
	L-SR1 1	42	11,643
$m = 5$	MSS Option 4	49	3,069
	L-SR1 BB	40	12,823
	L-SR1 1	44	12,928
$m = 7$	MSS Option 4	49	3,005
	L-SR1 BB	41	13,200
	L-SR1 1	43	11,660

Figure 3 contains the performance profile for total time needed to solve each problem for the case $m = 3$. From the profile, MSS with Option 4 takes significantly less time than either L-SR1 method. For the cases $m = 5$ and $m = 7$, the results are similar.

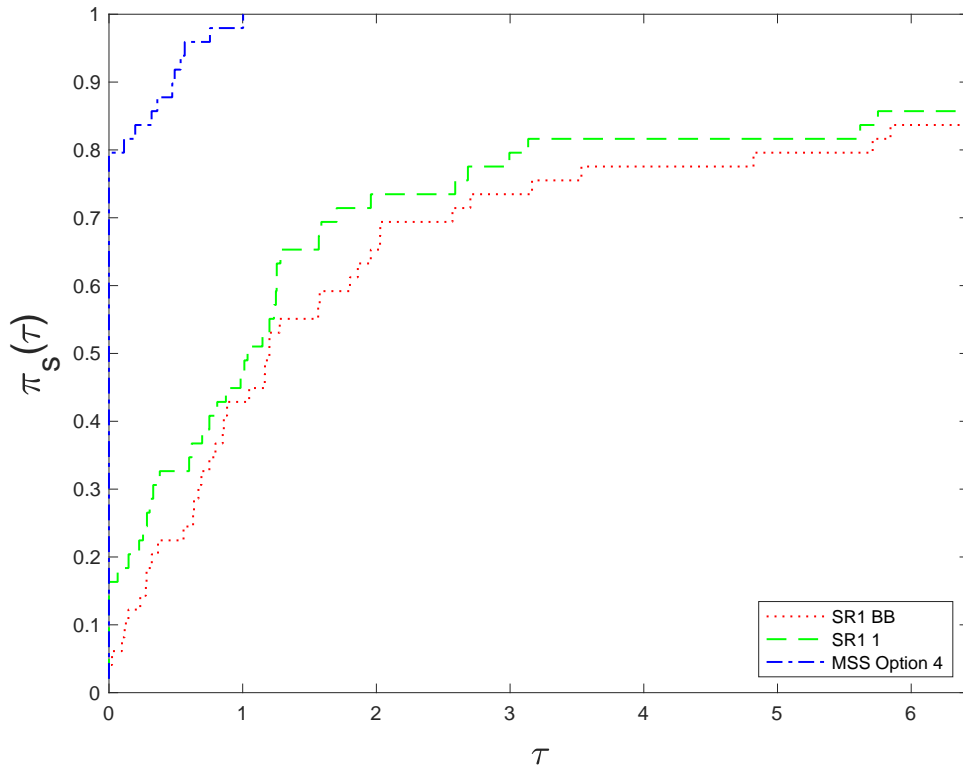


FIGURE 3. Performance profile comparing runtime using L-SR1 and MSS with $m = 3$. "SR1 BB" refers to using L-SR1 together with the BB initialization and "SR1 1" refers to using L-SR1 together with the initialization $B_0 = I$ each iteration.

Experiment 3. In this section, we compare the MSS method with a dense initialization to the limited-memory Powell-symmetric-Broyden (PSB) method. Similar to the MSS update, the PSB update is a rank-2 quasi-Newton update that can

generate indefinite Hessian approximations; thus, it is natural to use both methods in a trust-region framework. Moreover, PSB admits a compact representation [23] enabling us to use the same OBS-like solver that used for MSS. In other words, to use PSB, the only changes in Algorithm 1 for MSS that need to be made to use PSB are (i) the definition of M , (ii) the definition of Ψ , and (iii) the removal of the requirement that S is full rank in line 18. (For more details on the PSB update, see, e.g., [23].) For these experiments, a limited-memory PSB method was initialized using (i) $B_0 = \gamma_k I$, where $\gamma_k = (y_k^T y_k)/(s_k^T y_k)$ (i.e, the BB initialization) and (ii) $B_0 = \gamma_k I$, where $\gamma_k = (s_k^T y_k)/(s_k^T s_k)$, which is denoted as the "oBB" initialization in the table. Note that both these initialization are inspired by the results of (Theorem 3) with the stored vectors limited to the most current quasi-Newton pair (i.e., the number of stored pairs is one).

Figure 4–6 contains the performance profile for function evaluations. From the figure, it appears that MSS with Option 4 outperforms both implementations of L-PSB in terms of function evaluations using $m = 3$, $m = 5$, and $m = 7$, respectively. Table 6 lists cumulative results for these different memory sizes and initializations. To compute the total number of function evaluations in the table, only the problems on which all three methods using all three memory sizes were considered—this amounted to 45 problems. From the table, MSSM performs best on this test set for smaller memory sizes; in contrast, L-PSB with the BB initialization solved more problems with smaller memory sizes but the total number of function evaluations on the 45 problems was smallest with $m = 5$. Meanwhile, L-PSB with the oBB initialization performed better with larger memory sizes.

TABLE 6. Cumulative results on 49 CUTEst problems using MSS with Option 4 and L-PSB for various memory sizes. Here, "PSB BB" refers to using L-PSB together with the BB initialization and "PSB sBB" refers to using L-PSB together with the initialization $B_0 = (s_k^T y_k)/(s_k^T s_k)I$.

Memory	Solver	Problems solved	Function evaluations (FE)
$m = 3$	MSS Option 4	49	5927
	L-PSB BB	47	11,336
	L-PSB oBB	46	14,529
$m = 5$	MSS Option 4	49	6,290
	L-PSB BB	46	11,157
	L-PSB oBB	46	10,705
$m = 7$	MSS Option 4	49	6,648
	L-PSB BB	45	12,951
	L-PSB oBB	47	10,694

Finally, the performance profile for total runtime on the test set of 49 problems with $m = 3$ for MSS with Option 4 and the two PSB methods are found in Figure 7. This figure shows that MSS with Option 4 was the faster of the three methods on this test set.

6. CONCLUDING REMARKS

In this paper, we demonstrated how a dense initialization can be used with a MSS method. In numerical experiments on CUTEst test problems, the dense initialization

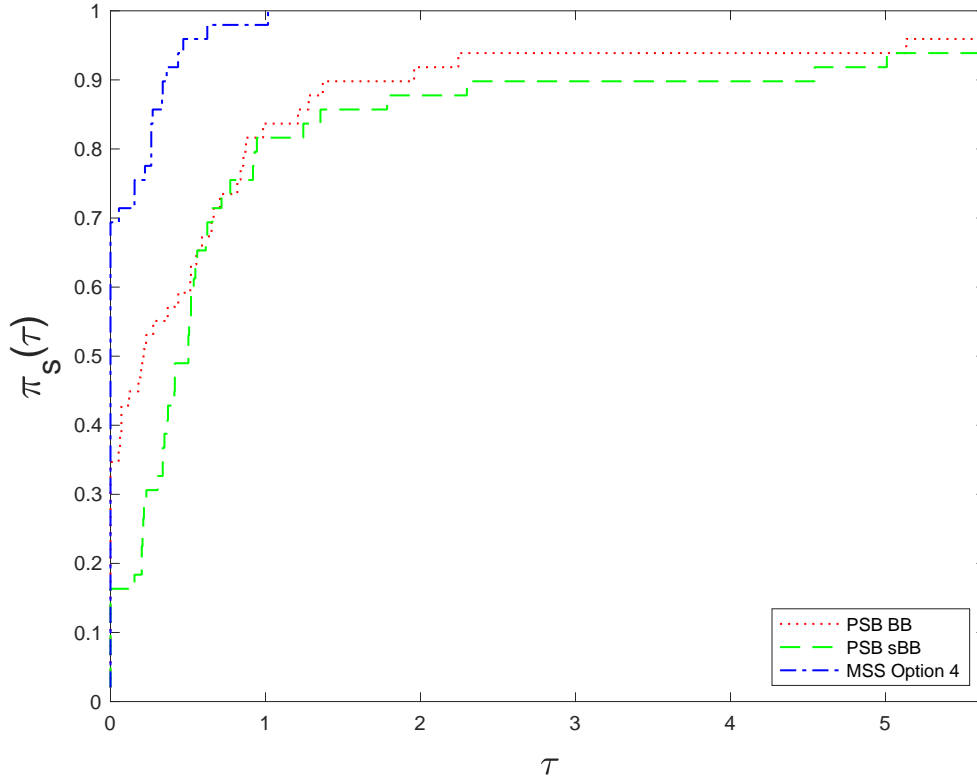


FIGURE 4. Performance profile comparing function evaluations using L-PSB and MSS with $m = 3$. "PSB BB" refers to using L-PSB together with the BB initialization and "PSB sBB" refers to using L-PSB together with the initialization $B_0 = (s_k^T y_k)/(s_k^T s_k)I$ each iteration.

performs better than standard constant diagonal initializations. Results suggest that this method performs well with small memory sizes (i.e., $m = 3$ outperformed the other memory sizes and the number of function evaluations generally increased as m increased). Moreover, with small m , the proposed method generally outperforms a basic L-SR1 trust-region method. Further research includes considering other symmetrization, choices for the two parameters ζ and ζ^C , and trust-region norms (including the so-called *shape-changing norm* first proposed in [24]). The results of future research will be submitted in subsequent papers.

6.1. Acknowledgement. The authors would like to thank the referees. In particular, one referee provided an explanation that led to the inclusion of Lemma 3 and significantly improved the entire section. In fact, part of the proof is based on an observation by the referee.

FUNDING

J. B. Erway's research work was funded by NSF Grant IIS-1741264.

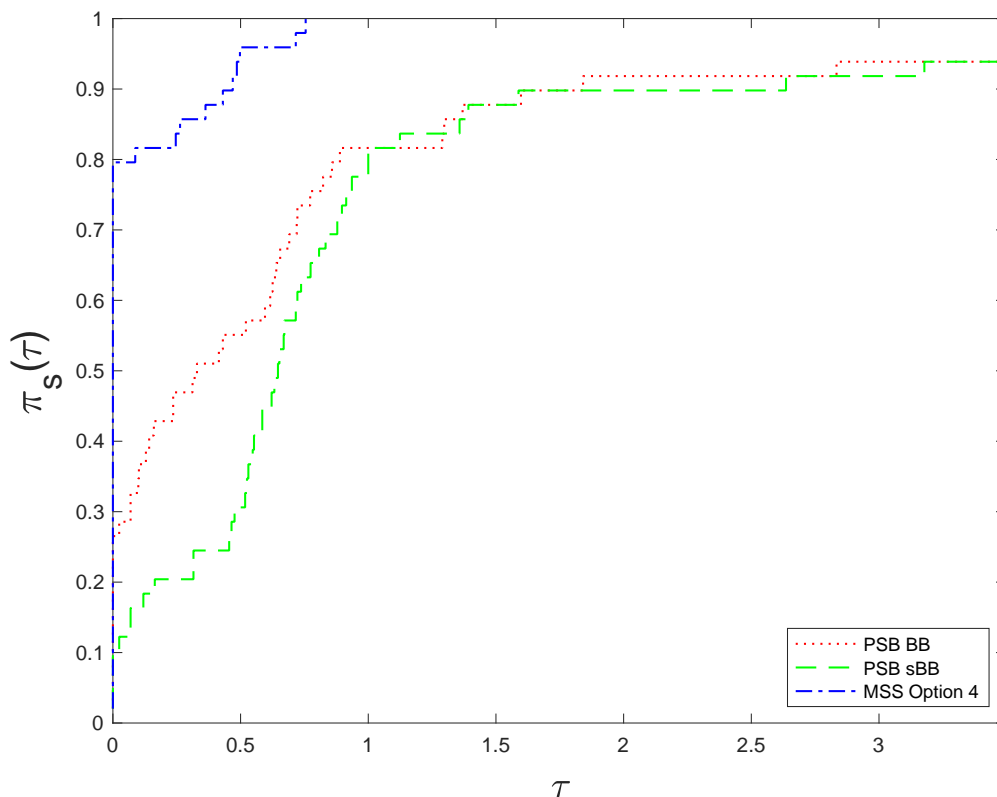


FIGURE 5. Performance profile comparing function evaluations using L-PSB and MSS with $m = 5$. "PSB BB" refers to using L-PSB together with the BB initialization and "PSB sBB" refers to using L-PSB together with the initialization $B_0 = (s_k^T y_k)/(s_k^T s_k)I$ each iteration.

REFERENCES

- [1] Oleg P Burdakov. Methods of the secant type for systems of equations with symmetric jacobian matrix. *Numerical functional analysis and optimization*, 6(2):183–195, 1983.
- [2] Oleg P Burdakov, José Mario Martínez, and Elvio A Pilotta. A limited-memory multipoint symmetric secant method for bound constrained optimization. *Annals of Operations Research*, 117(1-4):51–70, 2002.
- [3] Robert B Schnabel. Quasi-newton methods using multiple secant equations. Technical report, Colorado University at Boulder Department of Computer Science, 1983.
- [4] Johannes Brust, Oleg Burdakov, Jennifer B. Erway, and Roummel F. Marcia. A dense initialization for limited-memory quasi-Newton methods. *Computational Optimization and Applications*, 74(1):121–142, 2019.
- [5] Nicholas I. M. Gould, Dominique Orban, and Philippe L. Toint. Cutest: a constrained and unconstrained testing environment with safe threads for mathematical optimization. *Computational Optimization and Applications*, 60(3):545–557, 2015.
- [6] Johannes Joachim Brust. *Large-Scale Quasi-Newton Trust-Region Methods: High-Accuracy Solvers, Dense Initializations, and Extensions*. PhD thesis, UC Merced, 2018.
- [7] J. E. Dennis, Jr. and Jorge J. Moré. Quasi-newton methods, motivation and theory. *SIAM Review*, 19(1):46–89, 1977.
- [8] Richard H. Byrd, Jorge Nocedal, and Robert B. Schnabel. Representations of quasi-newton matrices and their use in limited memory methods. *Mathematical Programming*, 63(1):129–156, 1994.
- [9] Jorge Nocedal and Stephen Wright. *Numerical optimization*. Springer Science & Business Media, 2006.

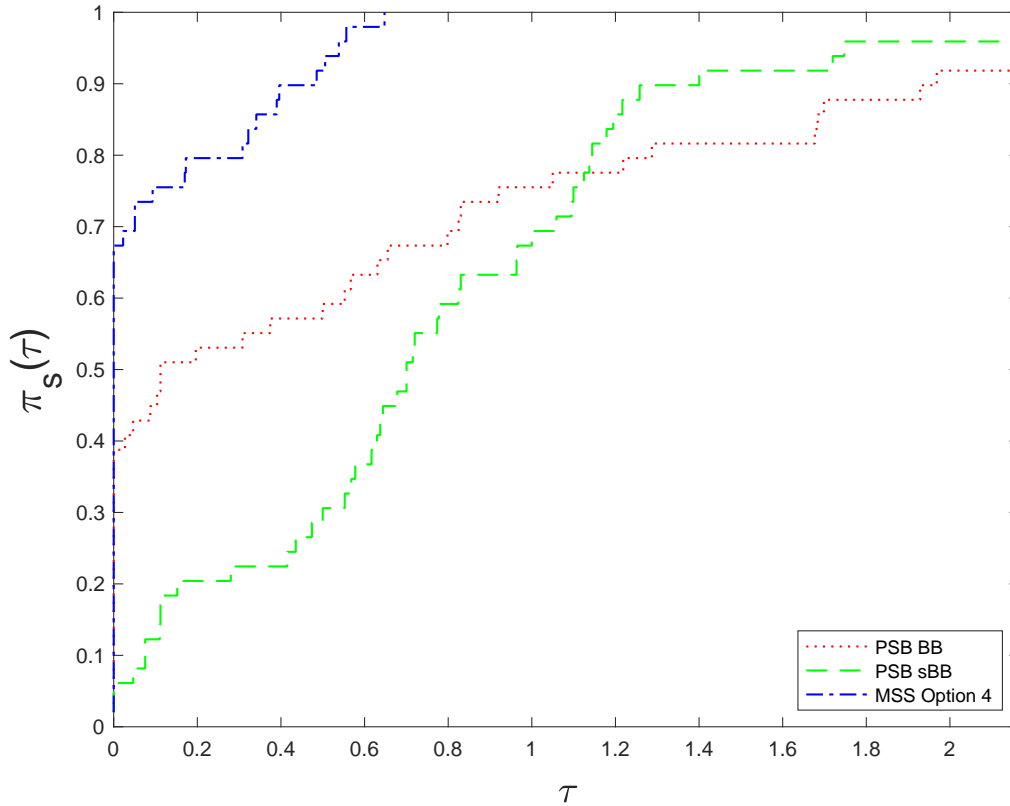


FIGURE 6. Performance profile comparing function evaluations using L-PSB and MSS with $m = 7$. Here, "PSB BB" refers to using L-PSB together with the BB initialization and "PSB sBB" refers to using L-PSB together with the initialization $B_0 = (s_k^T y_k)/(s_k^T s_k)I$.

- [10] Andrew R Conn, Nicholas IM Gould, and Philippe L Toint. *Trust region methods*. SIAM, 2000.
- [11] David M Gay. Computing optimal locally constrained steps. *SIAM Journal on Scientific and Statistical Computing*, 2(2):186–197, 1981.
- [12] Jorge J Moré and Danny C Sorensen. Computing a trust region step. *SIAM Journal on Scientific and Statistical Computing*, 4(3):553–572, 1983.
- [13] Jennifer B. Erway and Roummel F. Marcia. Algorithm 943: MSS: Matlab software for l-bfgs trust-region subproblems for large-scale optimization. *ACM Trans. Math. Softw.*, 40(4), 2014.
- [14] Oleg Burdakov, Lujin Gong, Spartak Zikrin, and Ya-xiang Yuan. On efficiently combining limited-memory and trust-region techniques. *Mathematical Programming Computation*, 9(1):101–134, 2017.
- [15] Johannes Brust, Jennifer B Erway, and Roummel F Marcia. On solving L-SR1 trust-region subproblems. *Computational Optimization and Applications*, 66(2):245–266, 2017.
- [16] Jennifer B Erway and Roummel F Marcia. On efficiently computing the eigenvalues of limited-memory quasi-Newton matrices. *SIAM Journal on Matrix Analysis and Applications*, 36:1338–1359, 2015.
- [17] Jonathan Barzilai and Jonathan M. Borwein. Two-point step size gradient methods. *IMA Journal of Numerical Analysis*, 8(1):141–148, 01 1988.
- [18] Johannes Brust, Oleg Burdakov, Jennifer Erway, and Roummel Marcia. Algorithm xxx: SC-SR1: MATLAB software for solving shape-changing L-SR1 trust-region subproblems. Technical report, arXiv:1607.03533 [math.OC], 2021.
- [19] Desmond J. Higham and Nicholas J. Higham. *MATLAB Guide*. SIAM, third edition, 2017.
- [20] Nicholas J. Higham. *Accuracy and Stability of Numerical Algorithms*. SIAM, 2nd edition, 2002.

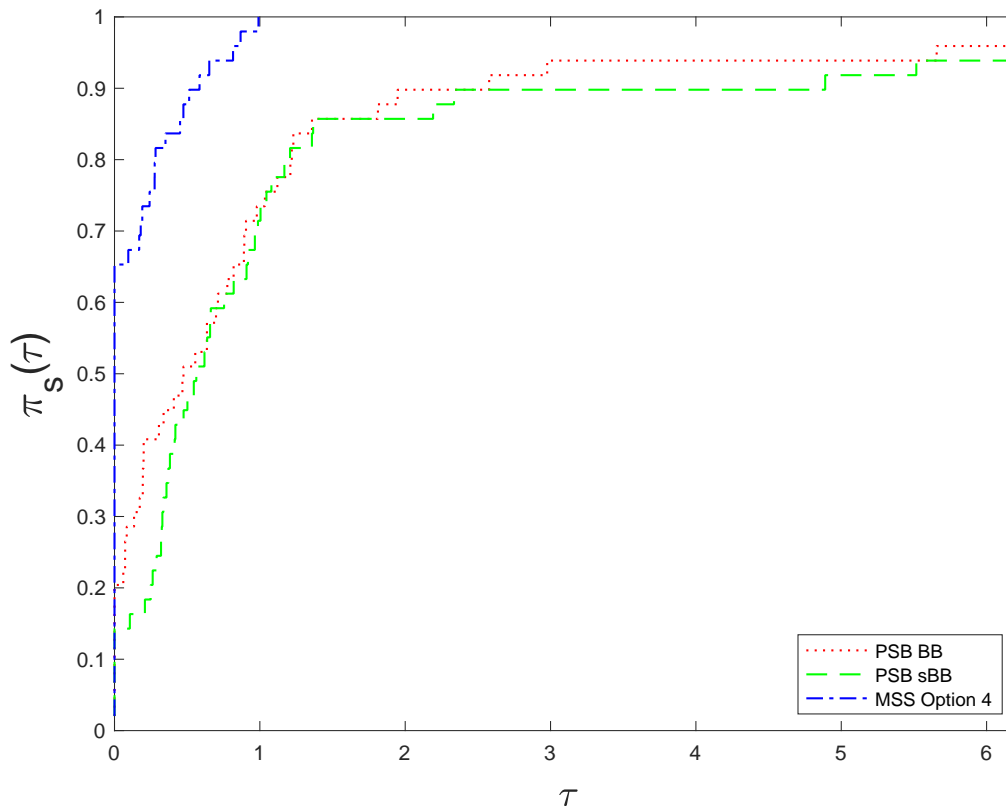


FIGURE 7. Performance profile runtime using L-PSB and MSS with $m = 3$. Here, "PSB BB" refers to using L-PSB together with the BB initialization and "PSB sBB" refers to using L-PSB together with the initialization $B_0 = (s_k^T y_k)/(s_k^T s_k)I$.

- [21] Jorge Nocedal. Updating quasi-newton matrices with limited storage. *Mathematics of Computation*, 35(151):773–782, 1980.
- [22] Elizabeth D. Dolan and Jorge J. Moré. Benchmarking optimization software with performance profiles. *Mathematical Programming*, 91:201–213, 2002.
- [23] Michael J.D. Powell. A new algorithm for unconstrained optimization. In J.B. Rosen, O.L. Mangasarian, and K. Ritter, editors, *Nonlinear Programming*, pages 31–65. Academic Press, 1970.
- [24] Oleg Burdakov and Ya-xiang Yuan. On limited-memory methods with shape changing trust region. In *Proceedings of the First International Conference on Optimization Methods and Software*, page p. 21, 2002.

Email address: erwayjb@wfu.edu

DEPARTMENT OF MATHEMATICS, WAKE FOREST UNIVERSITY, WINSTON-SALEM, NC 2 7109

Email address: rezapom@wfu.edu

DEPARTMENT OF MATHEMATICS, WAKE FOREST UNIVERSITY, WINSTON-SALEM, NC 2 7109